Check for updates

Received: 10 April 2023 | Revised: 30 July 2023 | Accepted: 3 August 2023

DOI: 10.1111/vru.13292

ORIGINAL RESEARCH

WILEY

Findings consistent with equine proximal suspensory desmitis can be reliably detected using computed tomography and differ between affected horses and controls

Eva M. T. Müller[1] | Katrien Vanderperren[2] | Roswitha Merle[3] | Svenja Rheinfeld[1] | Pitiporn Leelamankong[1] | Christoph J. Lischer[1] | Anna Ehrle[1]

[1]Equine Clinic, School of Veterinary Medicine, Freie Universität Berlin, Berlin, Germany

[2]Department of Medical Imaging of Domestic Animals and Orthopedics of Small Animals, Faculty of Veterinary Medicine, Ghent University, Merelbeke, Belgium

[3]Institute for Veterinary Epidemiology and Biostatistics, School of Veterinary Medicine, Freie Universität Berlin, Berlin, Germany

Correspondence
Eva M. T. Müller, Equine Clinic, School of Veterinary Medicine, Freie Universität Berlin, Oertzenweg 19 b, 14163 Berlin, Germany.
Email: e.mueller@fu-berlin.de

Oral presentation at the 32nd ECVS Annual Scientific Meeting in Cracow, Poland; July 6–8, 2023.

The objective of this retrospective, observational, controlled study was to evaluate bone and soft tissue window CT images of the proximoplantar metatarsus III region in twenty horses with pain localized to the proximal suspensory ligament (PSL) and 20 horses with findings nonrelated to tarsal pain. All horses underwent CT and radiographic examination. Images were reviewed by three independent observers who graded the severity and localization of findings. Bone-related categories as well as soft tissue-related categories were evaluated. For the comparison of imaging findings in horses with and without proximal suspensory desmitis (PSD), mixed linear regression was performed. The intraclass correlation coefficient (ICC) was calculated to assess intraobserver agreement, and kappa statistics were employed to evaluate interobserver agreement. CT examination identified significantly more abnormalities in the diseased group. The scores for osseous exostosis (p = .015) and PSL enlargement (p = .004) were notably higher in PSD horses compared to controls. Intraobserver agreement was overall high (ICC .82–1.0), and interobserver agreement was substantial for the detection of mineralization (kappa = .61) and moderate for sclerosis (kappa = .43), exostosis (kappa = .43), and PSL enlargement (kappa = .48/.51). Measurements in the soft tissue window were significantly smaller than those in the bone window. Findings concurrent with PSD including osseous proliferation and sclerosis as well as soft tissue enlargement, mineralization, and avulsion can be reliably detected using CT. Findings from the current study supported the use of CT for evaluating horses with suspected PSD where high-field MRI is not available.

KEYWORDS
advanced diagnostic imaging, hindlimb, lateral plantar nerve, ligament enlargement, proximal suspensory measurements

This is an open access article under the terms of the Creative Commons Attribution License, which permits use, distribution and reproduction in any medium, provided the original work is properly cited.
© 2023 The Authors. *Veterinary Radiology & Ultrasound* published by Wiley Periodicals LLC on behalf of American College of Veterinary Radiology.

1 | INTRODUCTION

Proximal suspensory desmitis (PSD) is an orthopedic condition commonly detected in sport horses.[1–3] The pathology is characterized by a varying combination of osseous changes at the proximoplantar metatarsus III (MTIII), enthesopathy, and desmopathy of the suspensory origin that may cause local nerve compression.[4–6] The diagnosis of PSD is generally based on regional analgesia and diagnostic imaging including ultrasonography and radiography.[5,7,8] It has, however, been shown that the majority of ultrasonographic measurements are not very precise and radiographic changes do not reliably predict the presence or severity of PSD.[6,9] High-field MRI is currently considered the most accurate imaging modality for the evaluation of the proximal suspensory ligament (PSL), but the technique is only available in a small number of referral centers.[11] Low-field MRI shows a detailed morphological correlation with the histological picture of PSD and is diagnostically relevant where other modalities fail to identify the reason for proximal MTIII pain.[10–14] The MRI pathological findings associated with PSD compared to the PSL origin in healthy horses are well described.[11–13,15]

The use of CT in equine orthopedic diagnostic imaging and particularly soft tissue imaging has significantly increased in recent years.[16–19] Particularly due to the short acquisition time and the increased availability of standing CT units at the referral level, CT imaging may offer a valid alternative to MRI of the PSL.[18–21] However, descriptions of CT findings at the level of the PSL origin in horses with and without PSD in the current literature are sparse.[22]

The objective of this study was to evaluate soft tissue and bone window CT images of the proximoplantar MTIII region in horses with and without proximal suspensory pain and to compare findings between observers with different levels of experience. The authors hypothesized that CT findings would differ for horses with versus without proximal suspensory pain and the intra- and interobserver repeatability for qualitative and quantitative CT findings would be high.

2 | METHODS

2.1 | Selection and description of subjects

For performing this retrospective, observational, controlled study, medical records (November 2019 to July 2022) were reviewed. Horses that underwent CT examination of the proximal metatarsus with proximal suspensory pain confirmed by deep branch analgesia were classified into the PSD group ($n = 20$). Age- and breed-matched horses that underwent CT examination of the proximal metatarsus and had no clinical signs of lameness localized to the tarsal joint or PSL were classified into the control group. Twenty horses were included in the PSD group and 20 horses in the control group. Images were reconstructed using a bone and soft tissue algorithm. All horses also underwent radiographic examination of the proximal metatarsus. Informed owner consent was obtained, and ethical approval was given by the local committee for research ethics (StN 007/23). Final decisions for the inclusion of horses in the study and classification of horses into the PSD group versus the control group were made by a Diplomate of the European College of Veterinary Surgery (ECVS), CertAVP VDI.

2.2 | Data recording and analysis

Full bone and soft tissue CT image series and radiographic images as well as transverse screenshots taken at levels 2, 4, and 6 cm distal to the tarsometatarsal joint (TMT) in both the bone and soft tissue CT algorithms were available. Images were blinded, randomized, and reviewed independently by a veterinary radiologist (diplomate of the European College of Veterinary Diagnostic Imaging), an equine veterinary surgeon (Diplomate ECVS), and a third-year resident (ECVS) without knowledge of group classification. Images were analyzed with the free and open-source code software program HOROS sponsored by Nimble Co LLC d/b/a Purview. Previously described grading systems for evaluation of radiographs (Rx) and MRI were modified to fit CT and radiographic assessment of the PSL (Supporting Information S1).[6,8,11,12]

The analysis of bone (B) and soft tissue window (ST) CT image series included the severity (grade 0–3) and localization of PSL findings (2/4/6 cm) with an evaluation of the following categories (Supporting Information S1):

- Distinction between muscle/fat/tendon in bone and soft tissue window (B/ST);
- Mottled heterogenous hypodense areas (B/ST);
- Definition of margins (B/ST);
- Mineralization within the PSL (B/ST);
- Adhesions between MTIII and PSL (B/ST);
- Distinction cortex/spongiosa (B/Rx);
- Endosteal sclerosis (B/Rx);
- Osseous resorption (B/Rx);
- Gullwing appearance (Rx);
- Fingerprint appearance (Rx);
- Osseous proliferation (B/Rx);
- Syndesmopathy (B/Rx);
- Avulsion fragment (B/Rx).

Findings were graded and their localization was documented in previously prepared templates (Figure 1). The maximum size of identified osseous spurs was measured (in mm) during bone window assessment.

Additionally, circumference PSL (mm), area PSL (mm^2) (B/ST), maximum thickness PSL (straight line, mm) (B/ST), and minimum distance MTIII to PSL (mm) (B/ST) were measured in the previously prepared transverse screenshots at 2, 4, and 6 cm distal to the TMT.

Based on the circumferential measurements, the overall PSL size was scored (mild enlargement: 280–350 mm^2; moderate: 350–370 mm^2; severe: >370 mm^2).[12] To assess intraobserver reliability, two reviewers (Diplomate ECVS, resident ECVS) repeated the measurements three times in 10 randomly selected image series.

17408261, 0, Downloaded from https://onlinelibrary.wiley.com/doi/10.1111/vru.13292 by EVIDENCE AID - BELGIUM, Wiley Online Library on [12/12/2023]. See the Terms and Conditions (https://onlinelibrary.wiley.com/terms-and-conditions) on Wiley Online Library for rules of use; OA articles are governed by the applicable Creative Commons License

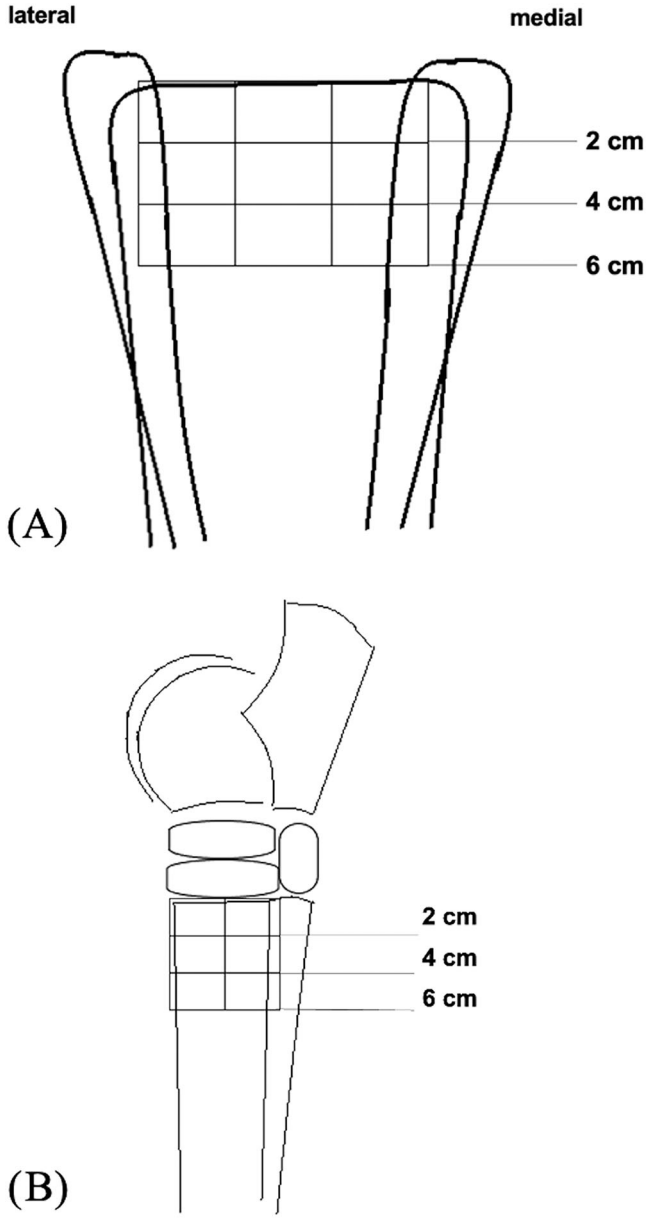

FIGURE 1 Template for documentation of computed tomographic findings in horses with and without proximal suspensory ligament desmitis: (A) Dorsoplantar view and (B) lateromedial view. Each grade (1–3) of finding was noted down in the small box within the template at the level of the exact location.

Additional findings were described by all reviewers separately. Tarsal bone pathologies were graded as mild, moderate, or severe. CT findings within the SL body and branches were summarized as enlargement and/or additional findings.

2.3 | Statistics

Data were stored in Microsoft Excel (Microsoft Excel 2022; Microsoft Corporation), and statistical analysis was performed with IBM SPSS (Version 25.0; IBM-SPSS Inc.). Statistical tests were selected by a Diplomate of the European College of Veterinary Public Health (ECVPH) and performed by a third-year resident ECVS. A power calculation was performed to determine the sample size. Generalized mixed linear regression was used to compare imaging findings in horses with and without PSD with the total score of findings as a categorial outcome, animal as a random factor, and group as a fixed factor. Differences between bone and soft tissue window measurements were calculated with the paired *t*-test for normally distributed data and with the Wilcoxon signed-rank test in case of nonnormal data distribution.

Mixed linear regression was utilized to determine the intraobserver reliability for continuous data. The respective parameter was used as the dependent variable, the animal ID as the fixed factor, and the measurement as the random factor. The intraclass correlation coefficient (ICC) was calculated as the percentage of variance within the measurements of one animal compared to the total variance. Small values indicate that there is not much variation between observers within one animal. For categorical data, Fleiss' kappa was used to analyze the interobserver reliability for all reviewers (for localization and severity of findings), while Cohen's kappa pairwise coefficient was used for comparisons between individual reviewers as well as for assessing differences between CT and Rx evaluations.[23] Descriptive analysis was performed for each evaluation, specifically involving 20 horses in the PSD group and 20 horses in the control group with a total of three evaluations—equivalent to one evaluation per reviewer ($n = 120$ for all evaluations, $n = 60$ for each group).

3 | RESULTS

3.1 | Horses

The following breeds were included: Warmbloods ($n = 27$), Pony ($n = 5$), Quarter Horse ($n = 2$), Arabian ($n = 2$), Irish Cob ($n = 2$), Draft breed ($n = 1$), and Friesian ($n = 1$). The mean body weight was 536 kg for the control horses (group A) and 590 kg for horses with PSD (group B). Control horses and horses with PSD were evenly distributed in three age groups: young, 2–9 years ($n = 13$); middle, 10–12 years ($n = 14$); senior, >13 years ($n = 13$). In the 40 horses included in the study, the overall age ranged from 2 to 19 years (mean age young: control group = 7 years and PSD group = 8 years; mean middle age: control group = 10 years and PSD group = 11 years; mean senior age: control group = 16 years and PSD group = 14 years). Eighteen left hindlimbs and 22 right hindlimbs were evaluated.

3.2 | CT imaging findings in horses with and without PSD

CT examination (32-detector-row scanner, Canon Aquilion One) was performed under general anesthesia. Computed tomographic parameters were as follows: 120 kVp, 400 mA, slice thickness of 1.25 mm, slice gap of 1.25 mm, field of view of 65 cm, with a matrix size of 512 × 512. The mean grades for all categories were higher in horses

17408261, 0, Downloaded from https://onlinelibrary.wiley.com/doi/10.1111/vru.13292 by EVIDENCE AID - BELGIUM, Wiley Online Library on [12/12/2023]. See the Terms and Conditions (https://onlinelibrary.wiley.com/terms-and-conditions) on Wiley Online Library for rules of use; OA articles are governed by the applicable Creative Commons License

TABLE 1 Mean values and 95% confidence interval of all categories in bone window and soft tissue window and radiographic assessment of horses with and without proximal suspensory desmitis.

	Mean values [95% confidence interval]	
Lesion categories	**Controls**	**PSD**
B-M/F/T	0.57 [0.39–0.75]	1.4 [1.14–1.66]
B-hypodense area	0.75 [0.56–0.94]	1.4 [1.17–1.63]
B-definition of margins (2 cm)	0.4 [0.23–0.57]	0.84 [0.58–1.10]
B-definition of margins (4 cm)	0.58 [0.40–0.77]	1.05 [0.81–1.30]
B-definition of margins (6 cm)	0.65 [0.46–0.84]	0.95 [0.70–1.19]
B-total mineralization	0.02 [0.00–0.05]	0.48 [0.26–0.70]
B-total adhesions	0.07 [0.00–0.14]	0.3 [0.13–0.47]
B-PSL enlargement[a]	0.2 [0.05–0.35]	0.93 [0.66–1.21]
B-distinction cortex/spongiosa	0.47 [0.31–0.62]	1.1 [0.89–1.31]
B-total endosteal sclerosis	0.55 [0.40–0.70]	1.12 [0.89–1.34]
B-total osseous resorption	0.87 [0.71–1.02]	1.13 [0.94–1.31]
B-total osseous proliferation[a]	0.73 [0.59–0.87]	1.6 [1.37–1.83]
B-total syndesmopathy[a]	0.4 [0.20–0.60]	1.4 [1.10–1.70]
B-total fragments	0.05 [0.00–0.12]	0.43 [0.24–0.63]
ST-M/F/T	0.37 [0.21–0.52]	1.35 [1.10–1.60]
ST-hypodense area	0.7 [0.54–0.86]	1.54 [1.31–1.77]
ST-definition of margins (2 cm)	0.23 [0.10–0.36]	0.74 [0.48–0.99]
ST-definition of margins (4 cm)	0.52 [0.36–0.68]	1.0 [0.73–1.27]
ST-definition of margins (6 cm)	0.58 [0.38–0.79]	1.05 [0.80–1.31]
ST-total mineralization	0.02 [0.00–0.05]	0.53 [0.30–0.77]
ST-total adhesions	0.11 [0.02–0.21]	0.32 [0.14–0.51]
ST-PSL enlargement	0.15 [0.03–0.27]	0.75 [0.47–1.02]
Rx-distinction cortex/spongiosa[a]	0.32 [0.17–0.46]	0.9 [0.67–1.13]
Rx-total endosteal sclerosis	0.63 [0.46–0.80]	1.18 [0.96–1.40]
Rx-total osseous resorption	0.28 [0.15–0.42]	0.7 [0.48–0.92]
Rx-Gullwing appearance	0.02 [0.00–0.05]	0.03 [0.00–0.08]
Rx-Fingerprint appearance[a]	0.1 [0.02–0.18]	0.25 [0.14–0.36]
Rx-total osseous proliferation	0.2 [0.05–0.35]	0.48 [0.23–0.73]
Rx-total fragments	0.02 [0.00–0.05]	0.07 [0.00–0.13]

Abbreviations: B, bone window; M/F/T, distinction between muscle/fat and tendon; PSL, proximal suspensory ligament; Rx, radiograph; ST, soft tissue window.
[a]Categories with significantly higher values in PSD group.

with PSD when compared to the control group (Table 1). The total grade for PSL enlargement ($p = .004$) (Figures 2A and 3), exostosis ($p = .015$) (Figure 2B), and syndesmopathy ($p = .001$) (Figure 2E) in the bone window assessment and the total grade for the distinction between cortex and spongiosa ($p = .016$) as well as the fingerprint appearance ($p = .04$) on radiographs were significantly higher in horses with PSD (Table 1).

3.2.1 | Specific soft tissue findings

PSL enlargement of grades 1–3 was identified in 55% (bone window) and 43.7% (soft tissue window) of cases in the PSD group (Tables 2 and 3). During bone window assessment, grades 2 and 3 were selected in 23.3% of screenshots at the level 2/4/6 cm distal to the TMT in the PSD group and in 5% of screenshots in the control group (Table 2). Thickness ($p = .007$–$.058$), as well as PSL area measurements ($p = .017$–$.056$), was significantly smaller in the control group when compared to the PSD group, with the exception of PSL area measurements (mm^2) ($p = .078$) at the 2 cm level in soft tissue window assessment. The mean PSL thickness was larger in all measurements of the PSD group at any evaluated level (Table 1). A PSL dorsoplantar thickness of >17.39 mm was seen in horses with PSD only. All soft tissue window measurements were significantly smaller ($p < .001$–$.026$) (e.g., area PSL measurement: 2 cm level = 11.7%; 4 cm level = 5.1%; and 6 cm level = 4.3%) than the measurements in the bone window, with the exception of the PSL thickness at 6 cm (Figures 4 and 5). The following PSL measurements

17408261, 0, Downloaded from https://onlinelibrary.wiley.com/doi/10.1111/vru.13292 by EVIDENCE AID - BELGIUM, Wiley Online Library on [12/12/2023]. See the Terms and Conditions (https://onlinelibrary.wiley.com/terms-and-conditions) on Wiley Online Library for rules of use; OA articles are governed by the applicable Creative Commons License

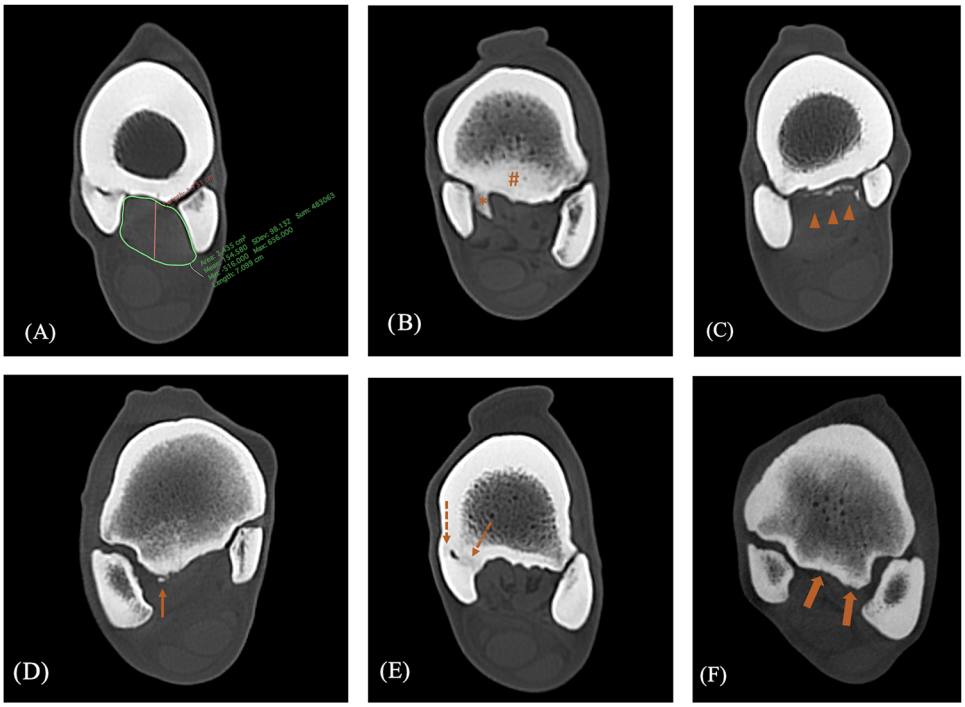

FIGURE 2 Bone window findings: (A) Orange line, maximum PSL thickness; green line, PSL circumference; (B) #, osseous sclerosis; *, osseous proliferation (exostosis); (C) arrowheads, mineralization; (D) arrow, avulsion fragment; (E) dotted arrows, syndesmopathy; (F) big orange arrows, osseous resorption; CT technical parameters: 120 kVp, 400 mA, slice thickness of 1.25 mm, slice gap of 1.25 mm, field of view of 65 cm, with a matrix size of 512 × 512. [Color figure can be viewed at wileyonlinelibrary.com]

TABLE 2 Total number and percentages of findings in computed tomographic bone window assessment of horses with and without proximal suspensory ligament desmitis.

Grade	0		1		2		3		Errors	
Pathology	Controls	PSD	Controls	PSD	Controls	PSD	Controls	PSD	Controls	PSD
M/F/T	33 (55%)	11 (18.3%)	20 (33.3%)	26 (43.3%)	7 (11.7%)	11 (18.3%)	0	12 (20%)	0	0
Hypodense area	25 (41.7%)	7 (11.7%)	26 (43.3%)	25 (41.7%)	8 (13.3%)	17 (28.3%)	1 (1.7%)	6 (10%)	0	5 (8.3%)
Total mineralization	59 (98.3%)	42 (70%)	1 (1.7%)	10 (16.7%)	0	5 (8.3%)	0	3 (5.0%)	0	0
Total adhesions	43 (71.7%)	29 (48.3%)	3 (5%)	11 (18.3%)	0	1 (1.7%)			14 (23.3%)	19 (31.7%)
Enlargement	52 (86.7%)	27 (45%)	5 (8.3%)	19 (31.7%)	2 (3.3%)	5 (8.3%)	1 (1.7%)	9 (15%)	0	0
Cortex/spongiosa	35 (58.3%)	13 (21.7%)	22 (36.7%)	32 (53.3%)	3 (5.0%)	11 (18.3%)	0	4 (6.7%)	0	0
Total sclerosis	30 (50%)	11 (18.3%)	27 (45%)	33 (55%)	3 (5.0%)	10 (16.7%)	0	5 (8.3%)	0	1 (1.7%)
Total resorption	15 (25%)	9 (15%)	38 (63.3%)	36 (60%)	7 (11.7%)	13 (21.7%)	0	2 (3.3%)	0	0
Total exostosis	19 (31.7%)	5 (8.3%)	38 (63.3%)	25 (41.7%)	3 (5.0%)	19 (31.7%)	0	11 (18.3%)	0	0
Total syn-desmopathy	43 (71.7%)	18 (30%)	13 (21.7%)	14 (23.3%)	1 (1.7%)	14 (23.3%)	3 (5.0%)	14 (23.3%)	0	0
Total fragment	58 (96.7%)	44 (73.3%)	1 (1.7%)	6 (10%)	1 (1.7%)	10 (16.7%)			0	0

Abbreviations: M/F/T, distinction between muscle/fat and tendon; PSD, proximal suspensory desmitis.

were significantly influenced by the horses' age: circumference/area PSL (mm/mm^2) (B/ST) (p = .009–.058) and maximum thickness PSL (B/ST) (p = .004–.049), with higher values observed in older horses of both groups. In the control group, the margins of PSL were graded between 0 and 2 in soft tissue and bone window assessment. In the PSD group, grade 3 was selected in 3.3% (2/60) to 8.3% (5/60) of CT image series.

The detection of adhesions remained difficult based on CT imaging. Sixty percent of all CT images in the bone window and 53.3% of the soft tissue-windowed images were evaluated for the presence of adhesions

17408261, 0, Downloaded from https://onlinelibrary.wiley.com/doi/10.1111/vru.13292 by EVIDENCE AID - BELGIUM, Wiley Online Library on [12/12/2023]. See the Terms and Conditions (https://onlinelibrary.wiley.com/terms-and-conditions) on Wiley Online Library for rules of use; OA articles are governed by the applicable Creative Commons License

TABLE 3 Total number and percentages of findings in computed tomographic soft tissue window assessment of horses with and without proximal suspensory ligament desmitis.

Grade	0		1		2		3		Errors	
Pathology	Controls	PSD	Controls	PSD	Controls	PSD	Controls	PSD	Controls	PSD
M/F/T	42 (70%)	11 (18.3%)	14 (23.3%)	27 (45%)	4 (6.7%)	12 (20%)	0	10 (16.7%)	0	0
Hypodense area	22 (36.7%)	5 (8.3%)	35 (58.3%)	25 (41.7%)	2 (3.3%)	18 (30%)	1 (1.7%)	9 (15%)	0	3 (5.0%)
Total mineralization	59 (98.3%)	42 (70%)	1 (1.7%)	7 (11.7%)	0	8 (13.3%)	0	3 (5.0%)	0	0
Total adhesions	40 (66.7%)	24 (40%)	5 (8.3%)	9 (15%)	0	1 (1.7%)			15 (25%)	26 (43.3%)
Enlargement	53 (88.3%)	34 (56.7%)	6 (10%)	13 (21.7%)	0	5 (8.3%)	1 (1.7%)	7 (11.7%)	0	1 (1.7%)

Abbreviations: M/F/T, distinction between muscle/fat and tendon; PSD, proximal suspensory desmitis.

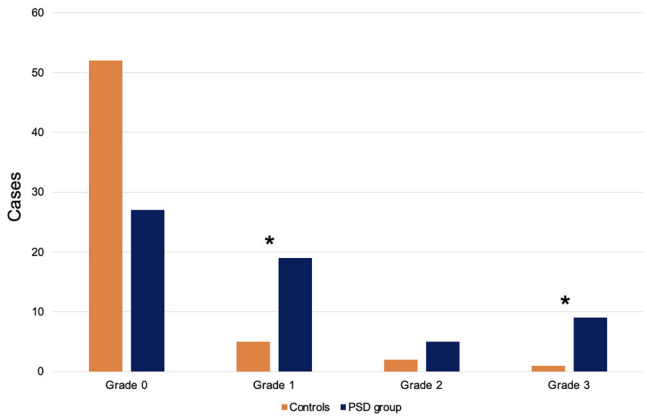

FIGURE 3 Total grade for enlargement of the proximal suspensory ligament (PSL) based on PSL area measurements (mm^2) in horses with proximal suspensory ligament desmitis (PSD) and controls as determined during bone window assessment. Grade 0, <280 mm^2; grade 1, 280–350 mm^2; grade 2, 350–370 mm^2; grade 3, >370 mm^2. *Significantly different values. [Color figure can be viewed at wileyonlinelibrary.com]

(Tables 2 and 3). Especially the less experienced reviewers stated that it was not possible to detect the presence of adhesions in the remaining images (Supporting Information S2). In horses with PSD, it was 2.9 times more likely that adhesions could not be assessed when compared to the control group (Tables 2 and 3).

Soft tissue mineralization graded between 1 and 3 was seen in bone and soft tissue windows in horses with PSD (30%). In the control group, 98.3% of CTs were graded as 0. There was only one horse with mineralization grade 1 in the control group. Mineralization in PSD horses was mainly detected on the plantaromedial aspect at the 4 cm level (8/18) (Tables 2 and 3).

Grades 2–3 mottled heterogenous hypodense areas in the PSL origin were identified more commonly in horses of the PSD group (B: 38.3%, 23/60; ST: 45%, 27/60) when compared to the controls (B: 15%, 9/60; ST: 5%, 3/60). Grade 1 mottled heterogenous hypodense areas in the PSL were diagnosed during bone window assessment (controls: 26/60 [43.3%]; PSD group: 25/60 [41.7%]) as well as soft tissue window assessment (controls: 35/60 [58.3%]; PSD group: 25/60 [41.7%]). The reviewers stated that it was not possible to assess the mottled heterogenous hypodense areas in 8.3% (B) and 5% (ST) of evaluations in the PSD group (Tables 2 and 3).

Additional findings within the SL body and SL branches were detected in 38 out of 120 (31.7%) of all evaluations. Twelve (10%) SL bodies and/or branches were described as subjectively enlarged. Additional findings were identified in 14 out of 120 (11.7%) SL bodies and/or branches. Both enlargement and additional findings were diagnosed in 12 out of 120 (10%) CT evaluations. In the control group, 10 (16.7%) CT evaluations were reported with SL body/branches subjective enlargement, seven (11.7%) with additional findings, and nine (15%) with both. In the PSD group, less additional findings within the SL body and branches were diagnosed: two (3.3%) with subjective enlargement, seven (11.7%) with additional findings, and three (5%) with both.

3.2.2 | Specific osseous findings

Osseous resorption (Figure 2F) was detected in 75% of CT evaluations in the control group with grade 1 = 63% and grade 2 = 11.7%. Grade 3 osseous resorption was detected in the PSD group only (3.3%), with grade 2 selected in 21.7% and grade 1 in 60% of cases in the PSD group (Table 2). In the PSD group, osseous resorption was mostly (57%) located in the proximal 2 cm of plantar MTIII (lateral [34/60] > medial [18/60]).

Moderate and severe syndesmopathy was identified more often in the PSD group (46.6%) compared to the controls (6.7%) (Table 2). In the PSD group, syndesmopathy was mostly located medially between MTII and MTIII (32/60).

Osteoarthritis of the tarsometatarsal joint (TMTJ), the distal intertarsal joint (DITJ), and the proximal intertarsal joint (PITJ) was detected in CT image series of the PSD and control group. In the control group, 26 CT images were diagnosed with mild osteoarthritis of the TMTJ, 20 of the DITJ, and six of the PITJ. Moderate osteoarthritis was detected in the TMTJ (1/60) and DITJ (9/60). Severe osteoarthritis of the TMTJ and DITJ was diagnosed in one CT evaluation in the control group. In the

17408261, 0, Downloaded from https://onlinelibrary.wiley.com/doi/10.1111/vru.13292 by EVIDENCE AID - BELGIUM, Wiley Online Library on [12/12/2023]. See the Terms and Conditions (https://onlinelibrary.wiley.com/terms-and-conditions) on Wiley Online Library for rules of use; OA articles are governed by the applicable Creative Commons License

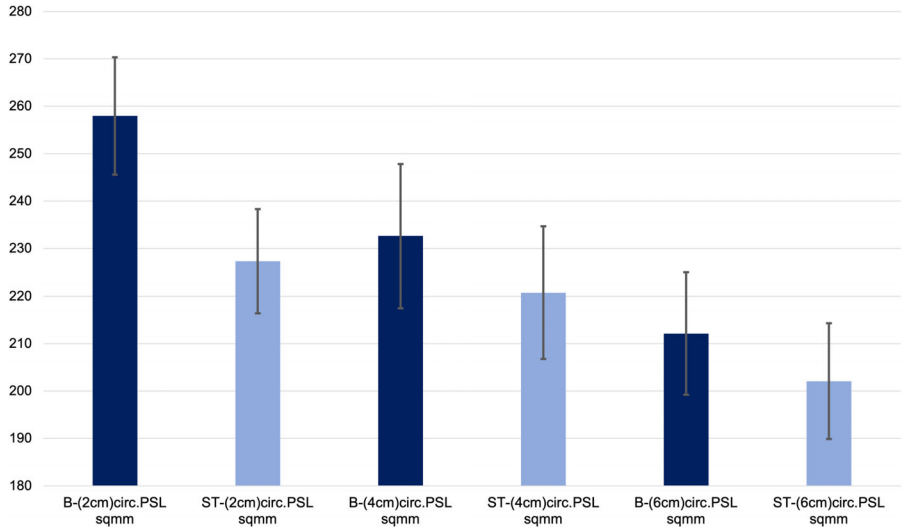

FIGURE 4 Comparison of proximal suspensory ligament area measurements (mm^2) in bone and soft tissue window at the different levels (2, 4, and 6 cm distal to the tarsometatarsal joint) in horses with proximal suspensory ligament desmitis and controls. The error bars illustrate the standard deviation. PSL, proximal suspensory ligament; B, bone window; ST, soft tissue window. [Color figure can be viewed at wileyonlinelibrary.com]

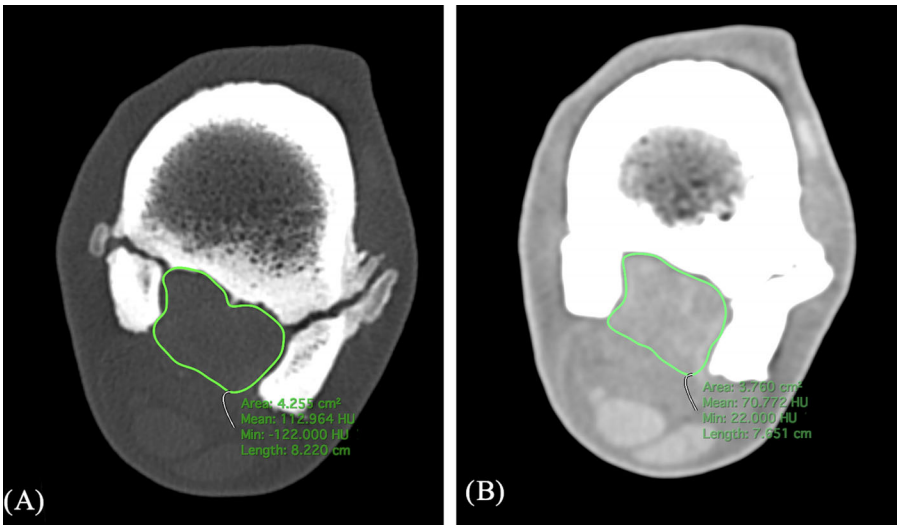

FIGURE 5 (A) Different proximal suspensory ligament area measurements in bone window (4.255 cm^2) (A) and soft tissue window (3.760 cm^2) (B) assessment at the same level; CT technical parameters: 120 kVp, 400 mA, slice thickness of 1.25 mm, slice gap of 1.25 mm, field of view of 65 cm, with a matrix size of 512 × 512. [Color figure can be viewed at wileyonlinelibrary.com]

PSD group, there were less CT images where mild osteoarthritis of the TMTJ (13/60) and DITJ (13/60) was described. Twelve CT evaluations were graded with mild PITJ osteoarthritis. Moderate osteoarthritis was identified in the DITJ (7/60) and PITJ (2/60). Severe osteoarthritis was diagnosed in the DITJ (1/60) and PITJ (1/60) in the PSD group. New bone formation on the distal tibia (lateral: controls [7/60], PSD group [8/60]; medial: controls [1/60], PSD group [1/60]; medial and lateral: PSD group [3/60]), osseous fragments at the distal intermediate ridge of the tibia (control group [6/60], PSD group [5/60]), cyst-like lesions in the talus (controls [2/60], PSD group [5/60]), and soft tissue swelling (PSD group [3/60]) were the most common additional findings. Further osseous findings are detailed in the following paragraph.

3.3 | Agreement between CT imaging and radiographic examination

Radiographic examination (Gierth HF 1000) was performed under sedation (dorsoplantar [70 kV, 3.2 mA]/lateromedial [64 kV, 5 mA] views). When comparing CT bone window and radiographic assessment, a moderate consensus was evident for endosteal sclerosis

17408261, 0, Downloaded from https://onlinelibrary.wiley.com/doi/10.1111/vru.13292 by EVIDENCE AID - BELGIUM, Wiley Online Library on [12/12/2023]. See the Terms and Conditions (https://onlinelibrary.wiley.com/terms-and-conditions) on Wiley Online Library for rules of use; OA articles are governed by the applicable Creative Commons License

TABLE 4 Total number and percentages of findings in radiographic assessment of horses with and without proximal suspensory desmitis.

Grade	0		1		2		3	
Pathology	Controls	PSD	Controls	PSD	Controls	PSD	Controls	PSD
Cortex/spongiosa	44 (73.3%)	23 (38.3%)	13 (21.7%)	24 (40%)	3 (5.0%)	9 (15%)	0	4 (6.7%)
Total sclerosis	28 (46.7%)	13 (21.7%)	26 (43.3%)	27 (45%)	6 (10%)	16 (26.7%)	0	4 (6.7%)
Total resorption	45 (75%)	32 (53.3%)	13 (21.7%)	16 (26.7%)	2 (3.3%)	10 (16.7%)	0	2 (3.3%)
Total exostosis	52 (86.7%)	46 (76.7%)	5 (8.3%)	4 (6.7%)	2 (3.3%)	5 (8.3%)	1 (1.7%)	5 (8.3%)
Total fragment	59 (98.3%)	56 (93.3%)	1 (1.7%)	4 (6.7%)	0	0		

Abbreviation: PSD, proximal suspensory desmitis.

(kappa = .511) and a fair agreement for the distinction between cortex and spongiosa (kappa = .298), as well as total exostosis (kappa = .237).

Endosteal sclerosis was seen in 65% of all CT evaluations. Twenty-five percent of CTs were graded with 2 and 3 in the PSD group. In the control group, grade 2 was identified only three times (5.0%) without any score for grade 3 (Table 2). On CT imaging, endosteal sclerosis was mostly seen in the proximal 2 cm on plantar MTIII in the PSD group.

During radiographic assessment, endosteal sclerosis was detected in 65.8% of evaluations. Thirty-three percent were graded with 2 and 3 in the PSD group. In the control group, grade 2 was identified in 10% of radiographs. The remaining radiographs were graded with 0 and 1 in the control group (Table 4).

The distinction between cortex and spongiosa was described as good less often in the PSD group (21.7%) when compared to the control group (58.3 %) on CT images (Table 2). During radiographic assessment, the distinction between cortex and spongiosa was good in 73.3% of controls but less so in the PSD group (38.3%) (Table 4).

Osseous proliferation was graded as 2 and 3 in 50% of all CT evaluations in the PSD group ($p = .015$). Grades 2 and 3 were identified in 5% of horses of the control group only (Table 2). Large osseous spurs >3.2 mm were solely seen in horses with PSD. Grade 1 osseous proliferations were identified in 63.3% of evaluations. In the PSD group, exostoses were mostly identified in the proximal 2 cm of MTIII (lateral [42/60] > medial [32/60]). During radiographic assessment, 23.3% of cases showed exostosis in the PSD group and 16.6% were graded 2 and 3 (Table 4).

Avulsion fragments were identified in 26.7% of CTs in the PSD group. In the control group, 3.3% of CT evaluations identified ($n = 1$) or suspected ($n = 1$) osseous fragments (Table 2). In the PSD group, most avulsion fragments were localized in the proximolateral 2 cm of MTIII on CT images. During radiographic evaluation, avulsion fragments were suspected in 6.7% of cases in the PSD group and in 1.7% in the control group (Table 4).

3.4 | Inter- and intraobserver reliability

There was substantial agreement between reviewers for the detection of soft tissue mineralization (85%) (Figure 2C) in bone window assessment (benchmarks: .61–.80). Moderate (benchmarks: .41–.60) agreement was evident for the detection of B-endosteal sclerosis (50%) (Figure 2B), B/ST-PSL enlargement (70%) (Figure 2A), and B-osseous proliferation (42.5%) (Figure 2B).

B-avulsion fragment (Figure 2D), B-distinction cortex/spongiosa, B/ST-distinction muscle/fat/tendon, B-syndesmopathy (Figure 2E), and Rx-osseous resorption were recorded with fair (benchmarks: .21–.40) agreement between reviewers. Pairwise comparison indicated a more substantial agreement in several categories (Supporting Information S2). The measurements for B/ST-2 cm area PSL (mm^2) ($p = .055/.97$) showed the highest agreement between reviewers.

The overall intraobserver reliability for the detection of findings and grading as well as the given measurements was high (ICC .82–1.0). PSL circumferential measurements (mm) (ICC .58) in the soft tissue window and measuring the distance between PSL and MTIII in the bone window (ICC .64) at the 4 cm level were the least accurate.

4 | DISCUSSION

Findings that support the authors' hypothesis were that based on area and thickness measurements, significantly more PSL enlargement, as well as osseous exostosis, was identified in horses with PSD.

An initial report introducing CT evaluation in three horses with PSD already described new bone formation at the level of the proximopalmar/proximoplantar MTIII.[22] In agreement with this report, large osseous spurs (>3.2 mm) extending from the level of proximoplantar MTIII were detected in PSD horses only and are generally underestimated during radiographic assessment. Osseous proliferations were commonly detected on the lateral aspect in the proximal 2 cm of the plantar MTIII. A retrospective radiographic study describes increased radiopacity to be significantly more prevalent on lateral MTIII in horses with hindlimb PSD.[8] Mild osseous proliferations were also identified in the control group in the current study. This observation may reflect new bone formation due to physiological load inflicted by the inserting fibers of the suspensory origin.[8] A recent report comparing radiographic images with MRI as a gold standard confirmed the presence of radiographic findings at proximal MTIII in horses with PSD. It was, however, pointed out that radiographic changes should be interpreted with caution as the presence and severity of PSD cannot be predicted based on radiographic examination alone.[6]

In line with MRI evaluation, soft tissue mineralization was predominantly detected in horses with PSD during CT imaging, with only one

17408261, 0, Downloaded from https://onlinelibrary.wiley.com/doi/10.1111/vru.13292 by EVIDENCE AID - BELGIUM, Wiley Online Library on [12/12/2023]. See the Terms and Conditions (https://onlinelibrary.wiley.com/terms-and-conditions) on Wiley Online Library for rules of use; OA articles are governed by the applicable Creative Commons License

horse in the control group showing mild soft tissue mineralization grade 1.[12] Additionally, avulsion fragments were identified particularly at the planterolateral aspect proximal MTIII at the level of the inserting PSL fibers in horses with PSD.[10] Both soft tissue mineralization and avulsion fragments were underdiagnosed during radiographic examination.

The increased total score for PSL enlargement in horses with PSD supports the theory that PSL enlargement may cause compartment syndrome with irritation of the deep branch of the lateral plantar nerve.[24] In the present study, the mean PSL area (mm^2) was consistently higher in the PSD group than in the controls. In contrast, MRI evaluation of the PSL size did not confirm a significant increase in size in horses with PSD.[12] To further validate this discrepancy, a study comparing PSL measurements in CT and MRI imaging would be of great interest.

Variations in measurements have been described for the ultrasonographic assessment of the PSL.[9] The current study identified high intraobserver reliability for the majority of measurements. The interobserver reliability was higher during the bone window assessment when compared to the soft tissue window. Additionally, soft tissue window measurements ($p < .001$–$.026$) were significantly smaller when compared to bone window analysis. The reason for this observation is most likely based on the different window settings between bone and soft tissue windows. The adjacent bone appears brighter and thicker in the soft tissue window. The mean PSL thickness was larger in all measurements of the PSD group at all levels evaluated. Measurements >17.39 mm were only detected in horses with PSD. The measurement of the dorsopalmar/dorsoplantar PSL thickness has been shown to be the most precise during the ultrasonographic examination of the PSL. Area PSL measurement at the 2 cm level was the most reliable measurement in the current study. The authors would therefore recommend performing measurements 2 cm distal to the TMTJ.[9]

Osseous resorption was diagnosed in 85% of the PSD group as well as in 75% of controls. Mild osseous resorption (grade 1) was diagnosed comparably often in the controls compared to the PSD group. This observation suggests that anatomic variations are present in horses, especially in the proximal 2 cm of plantar MTIII. Similarly, grade 1 mottled heterogenous hypodense areas in the PSL were diagnosed during bone window assessment as well as soft tissue window assessment in both groups, reflecting the anatomically heterogenous appearance of the PSL at this level.[24]

Due to the clinical character of this research, a limitation of the study is the lack of comparison to a gold standard like high-field MRI or histology. A limitation of CT evaluation of the PSL appears to be the detection of adhesion formation between the PSL and plantar MTII—MTIV. During MRI evaluation, the presence of adhesion has been proposed to be a main criterion for a PSD diagnosis in one study.[11]

Proximal suspensory pain was confirmed by a positive deep branch analgesia of the lateral plantar nerve. It is highly recommended to scrutinize the results of local analgesia due to the possibility of proximal diffusion and inadvertent intrasynovial injection.[25] A limitation of this study is that intrasynovial analgesia was inconsistently performed for confirmation.

In conclusion, CT imaging can reliably detect findings concurrent with PSD including osseous proliferation and sclerosis as well as soft tissue enlargement, mineralization, and avulsion fragments. Findings from the current study supported the use of CT for evaluating horses with suspected PSD where high-field MRI is not available.

ACKNOWLEDGMENTS

The authors would like to thank the support staff involved in the horses' examination. STROBE checklist was considered for the preparation of the manuscript.

LIST OF AUTHOR CONTRIBUTIONS

Category 1

a. **Conception and Design**: Müller, Vanderperren, Lischer, Ehrle
b. **Acquisition of Data**: Müller, Rheinfeld, Leelamankong
c. **Analysis and Interpretation of Data**: Müller, Merle, Ehrle

Category 2

a. Drafting the Article: Müller, Ehrle
b. Revising Article for Intellectual Content: Müller, Vanderperren, Merle, Lischer, Rheinfeld, Leelamankong, Lischer, Ehrle

Category 3

a. **Final Approval of Completed Article**: Müller, Vanderperren, Merle, Rheinfeld, Leelamankong, Lischer, Ehrle

Category 4

a. Agreement to be accountable for all aspects of the work in ensuring that questions related to the accuracy or integrity of any part of the work are appropriately investigated and resolved: Müller, Vanderperren, Merle, Rheinfeld, Leelamankong, Lischer, Ehrle

CONFLICT OF INTEREST STATEMENT

The authors declare no conflicts of interest.

DATA AVAILABILITY STATEMENT

The data acquired during this study are available from the corresponding author upon request.

REFERENCES

1. Gibson KT, Steel CM. Conditions of the suspensory ligament causing lameness in horses. *Equine Vet Educ*. 2002;14(1):39-50. doi:10.1111/j.2042-3292.2002.tb00137.x
2. Meehan L, Labens R. Diagnosing desmitis of the origin of the suspensory ligament. *Equine Vet Educ*. 2016;28(6):335-343. doi:10.1111/eve.12331
3. Gruyaert M, Pollard D, Dyson SJ. An investigation into the occurrence of, and risk factors for, concurrent suspensory ligament injuries in horses with hindlimb proximal suspensory desmopathy. *Equine Vet Educ*. 2020;32:173-182. doi:10.1111/eve.13187
4. Toth F, Schumacher J, Schramme M, Holder T, Adair HS, Donnell RL. Compressive damage to the deep branch of the lateral plantar nerve

17408261, 0, Downloaded from https://onlinelibrary.wiley.com/doi/10.1111/vru.13292 by EVIDENCE AID - BELGIUM, Wiley Online Library on [12/12/2023]. See the Terms and Conditions (https://onlinelibrary.wiley.com/terms-and-conditions) on Wiley Online Library for rules of use; OA articles are governed by the applicable Creative Commons License

associated with lameness caused by proximal suspensory desmitis. *Vet Surg*. 2008;37(4):328-335. doi:10.1111/j.1532-950X.2008.00385.x
5. Dyson S, Murray R, Pinilla MJ. Proximal suspensory desmopathy in hindlimbs: a correlative clinical, ultrasonographic, gross post mortem and histological study. *Equine Vet J*. 2017;49(1):65-72. doi:10.1111/evj.12563
6. Hinkle FE, Selberg KT, Frisbie DD, Barrett MF. Radiographic changes of the proximal third metatarsal bone do not predict presence or severity of proximal suspensory desmopathy in a predominately Quarter Horse population. *Equine Vet J*. 2023;55(1):24-32. doi:10.1111/evj.13562
7. Hinnigan G, Milner P, Talbot A, Singer E. Is anaesthesia of the deep branch of the lateral plantar nerve specific for the diagnosis of proximal metatarsal pain in the horse? *Vet Comp Orthop Traumatol*. 2014;27(5):351-357. doi:10.3415/VCOT-13-12-0146
8. Trump M, Siegenthaler E, Kircher PR, Furst A, Theiss F. Comparison of radiographic changes of the proximal third metacarpal and metatarsal bones in horses with and without proximal suspensory desmitis. *Pferdeheilkunde*. 2014;30(6):671-676. doi:10.5167/uzh-100034
9. Zauscher JM, Estrada R, Edinger J, Lischer CJ. The proximal aspect of the suspensory ligament in the horse: how precise are ultrasonographic measurements? *Equine Vet J*. 2013;45(2):164-169. doi:10.1111/j.2042-3306.2012.00597.x
10. Bischofberger AS, Konar M, Ohlertht S, et al. Magnetic resonance imaging, ultrasonography and histology of the suspensory ligament origin: a comparative study of normal anatomy of Warmblood horses. *Equine Vet J*. 2006;38(6):508-516. doi:10.2746/042516406X156109
11. Labens R, Schramme MC, Robertson ID, Thrall DE, Redding WR. Clinical, magnetic resonance, and sonographic imaging findings in horses with proximal plantar metatarsal pain. *Vet Radiol Ultrasound*. 2010;51(1):11-18. doi:10.1111/j.1740-8261.2009.01614.x
12. van Veggel E, Selberg K, van der Velde-Hoogelander B, Bolas N, Vanderperren K, Bergman HJ. *Magnetic resonance imaging findings of the proximal metacarpal region in warmblood horses: 36 lame and 26 control limbs (2015-2021)*. 2021;8:714423. doi:10.3389/fvets.2021.714423
13. Barrett MF, Selberg KT, Johnson SA, Hersman J, Frisbie DD. High field magnetic resonance imaging contributes to diagnosis of equine distal tarsus and proximal metatarsus lesions: 103 horses. *Vet Radiol Ultrasound*. 2018;59(5):587-596. doi:10.1111/vru.12659
14. Schramme M, Josson A, Linder K. Characterization of the origin and body of the normal equine rear suspensory ligament using ultrasonography, magnetic resonance imaging, and histology. *Vet Radiol Ultrasound*. 2012;53(3):318-328. doi:10.1111/j.1740-8261.2011.01922.x
15. Dyson S, Pinilla MJ, Bolas N, Murray R. Proximal suspensory desmopathy in hindlimbs: magnetic resonance imaging, gross post-mortem and histological study. *Equine Vet J*. 2018;50(2):159-165. doi:10.1111/evj.12756
16. Vallance SA, Bell RJ, Spriet M, Kass PH, Puchalski SM. Comparison of computed tomography, contrast-enhanced computed tomography and standing low-field magnestic resonance imaging in horses with lameness localised to the foot. Part 2: lesion identification. *Equine Vet J*. 2012;44(2):149-156. doi:10.1111/j.2042-3306.2011.00386.x
17. Riggs CM. Computed tomography in equine orthopaedics—the next great leap? *Equine Vet Educ*. 2019;31(3):151-153. doi:10.1111/eve.12885
18. Mathee N, Robert M, Higgerty SM, et al. Computed tomographic evaluation of the distal limb in the standing sedated horse: technique, imaging diagnoses, feasibility, and artifacts. *Vet Radiol Ultrasound*. 2022;64(2):243-252. doi:10.1111/vru.13182
19. Mageed M. Standing computed tomography of the equine limb using a multi-slice helical scanner: technique and feasibility study. *Equine Vet Educ*. 2022;34(2):77-83. doi:10.1111/eve.13388
20. Koch C, Pauwels F, Schweizer D. Technical set-up and case illustrations of orthopaedic cone beam computed tomography in the standing horse. *Equine Vet Educ*. 2020;33(5):255-262. doi:10.1111/eve.13290
21. Brounts SH, Lund JR, Whitton RC, Ergun DL, Muir P. Use of a novel helical fan beam imaging system for computed tomography of the distal limb in sedated standing horses: 167 cases (2019-2020). *J Am Vet Med Assoc*. 2022;260(11):1351-1360. doi:10.2460/javma.21.10.0439
22. Launois MT, Vandeweerd JM, Perrin RA, Brogniez L, Desbrosse FG, Clegg PD. Use of computed tomography to diagnose new bone formation associated with desmitis of the proximal aspect of the suspensory ligament in third metacarpal or third metatarsal bones of three horses. *J Am Vet Med Assoc*. 2009;234(4):514-518. doi:10.2460/javma.234.4.514
23. Landis JR, Koch GG. The measurement of observer agreement for categorical data. *Biometrics*. 1977;33(1):159-174. doi:10.2307/2529310
24. Dyson SJ. Proximal metacarpal and metatarsal pain: a diagnostic challenge. *Equine Vet Educ*. 2003;15(3):134-138. doi:10.1111/j.2042-3292.2003.tb00231.x
25. Claunch KM, Eggleston RB, Baxter GM. Effects of approach and injection volume on diffusion of mepivacaine hydrochloride during local analgesia of the deep branch of the lateral plantar nerve in horses. *J Am Vet Assoc*. 2014;245(10):1153-1159. doi:10.2460/javma.245.10.1153

SUPPORTING INFORMATION

Additional supporting information can be found online in the Supporting Information section at the end of this article.

How to cite this article: Müller EMT, Vanderperren K, Merle R, et al. Findings consistent with equine proximal suspensory desmitis can be reliably detected using computed tomography and differ between affected horses and controls. *Vet Radiol Ultrasound*. 2023;1-10. https://doi.org/10.1111/vru.13292

17408261, 0, Downloaded from https://onlinelibrary.wiley.com/doi/10.1111/vru.13292 by EVIDENCE AID - BELGIUM, Wiley Online Library on [12/12/2023]. See the Terms and Conditions (https://onlinelibrary.wiley.com/terms-and-conditions) on Wiley Online Library for rules of use; OA articles are governed by the applicable Creative Commons License